Journal of Rice Research and Developments

Research Article DOI: 10.36959/973/449

Struvite Effects on Greenhouse Gas Emissions from Furrow-irrigated Rice in the Greenhouse

Chandler M Arel^{1*}, Kristofor R Brye², Diego Della Lunga³, Trenton L Roberts⁴ and Richard Adams⁵



¹Instructor, Department of Crop, Soil, and Environmental Sciences, University of Arkansas, USA

²University Professor, Department of Crop, Soil, and Environmental Sciences, University of Arkansas, USA

³Post-Doctoral Fellow, Department of Crop, Soil, and Environmental Sciences, University of Arkansas, USA

⁴Professor, Department of Crop, Soil, and Environmental Sciences, University of Arkansas, USA

⁵Assistant Professor, Department of Entomology and Plant Pathology, University of Arkansas, USA

Abstract

The production and use of struvite (MgNH,PO, 6H,O) as an alternative fertilizer-phosphorus (P) source could remove excess nutrients from wastewater and potentially reduce greenhouse gas (GHG) emissions from agricultural production systems such as furrow-irrigated rice. The objective of this study was to evaluate the effects of fertilizer-P source [i.e., synthetic and real-wastewater-derived electrochemically precipitated struvite (ECST_{syn} and ECST_{Real}, respectively), chemically precipitated struvite (CPST), monoammonium phosphate (MAP), and an unamended control (UC)] on carbon dioxide (CO₂), methane (CH₄), and nitrous oxide (N₂O) fluxes, season-long emissions, and global warming potentials (GWPs) from simulated furrow-irrigated rice. The hybrid rice cultivar RT 7302 was grown in tubs under controlled greenhouse conditions in a P-deficient silt-loam soil. Gas sample collection occurred weekly over a 162-day period during Summer 2023. Season-long emissions and GWPs were calculated at the end of the season. Season-long N₂O emissions were greatest from the UC (6.1 kg N₂O ha⁻¹ season⁻¹) and differed from all other fertilizer-P treatments. Season-long CO, emissions were similar among P-receiving treatments but were numerically greatest from MAP (23.2 Mg CO, ha-1 season⁻¹), which was similar to CPST and both ECST fertilizer-P sources. The CO₂-excluded GWP was greatest from the UC (1622.7 kg CO₂-equivalents ha⁻¹ season⁻¹) and differed from all other fertilizer-P treatments. Results of this study emphasized that the use of wastewater-recovered struvite in furrow-irrigated rice could improve the sustainability of Arkansas rice production through the reduction of GHG emissions without reducing plant response compared to other widely used, commercially available fertilizer-P sources.

Keywords

Electrochemically precipitated struvite, Greenhouse gases, Furrow-irrigated rice, Phosphorus

Introduction

Over the past 45 years, the reduced supply of mineable phosphorus (P), the increasing of atmospheric greenhouse gas (GHG) concentrations and the related intensification of climate change have raised global concerns and directed scientific focus on how to improve the sustainability of P and reduce GHG emissions in agricultural systems [1,2]. Since 1988, the Intergovernmental Panel on Climate Change (IPCC) has released six assessments on climate change and its anthropogenic roots, that have led to the establishment of international policies focused on limiting the expected rise in global air temperatures through the reduction of GHG emissions, namely methane (CH_4) , nitrous oxide (N_2O) , and carbon dioxide (CO_2) , from key sources in

industry, transportation, and agriculture [2]. Simultaneously, international research efforts have sought to improve P sustainability in agriculture by progressing research on

*Corresponding author: Chandler M Arel, Instructor, Department of Crop, Soil, and Environmental Sciences, University of Arkansas, 115 Plant Sciences Building, Fayetteville, AR 72701, USA

Accepted: June 21, 2025

Published online: June 25, 2025

Citation: Arel CM, Brye KR, Lunga DD, et al. (2025) Struvite Effects on Greenhouse Gas Emissions from Furrow-irrigated

Rice in the Greenhouse. J Rice Res Dev 7(1):491-503

Copyright: © 2025 Arel CM, et al. This is an open-access article distributed under the terms of the Creative Commons Attribution License, which permits unrestricted use, distribution, and reproduction in any medium, provided the original author and source are credited.



irrigation water and nutrient management and alternative fertilizer-P sources, as the demand for P fertilizers for agricultural production has increased over time and is expected to continue to increase into the future, but with a finite supply of mineable rock phosphate [1].

Currently, agricultural sources represent ~11% of GHG emissions within the United States (US), which is expected to increase into the future as the production of agricultural products increases to meet the demand of increasing global human population [1,3]. As a result of population growth, the International Water Management Institute estimated that global food production must grow by 70% by 2050 to provide an adequate supply of high-quality calories [4]. Within agriculture, the majority of GHGs are emitted from enteric fermentation, manure, rice cultivation, agricultural soil management, liming, urea fertilization, and field burning [3]. An increase in agricultural production would likely result in an increase in CO₂, CH₄, and N₂O emissions, as the conditions present in agricultural soils often encourage the release of GHGs by providing favorable conditions for the processes of methanogenesis, nitrification, denitrification, and respiration [5,6].

Soil respiration is responsible for CO, production and release into the atmosphere, as aerobic, heterotrophic microbes decompose soil organic matter (SOM) and as roots release CO₂ [5]. Methane production in the soil occurs as microbes, mainly methanogens, use C as a terminal electron acceptor during SOM decomposition in anaerobic conditions [7]. Enteric fermentation and the management of manure were the primary sources of anthropogenic CH, production in 2020, representing 36.1% of all CH_4 emissions in the US [3]. Denitrifying, chemoorganotrophic bacteria in the soil, anaerobically convert nitrate (NO₃-) into nitrite (NO₃-) and then into either nitric oxide (NO), N2O, or dinitrogen gas (N₂) [5]. In contrast to CH₄, the majority of N₂O emissions are attributed to agricultural soil management (74.2%) via fertilizer applications that are then denitrified [3]. The production of CO₂, CH₄, and N₂O is influenced greatly by the conditions present in the soil, and by nutrient and irrigation management practices.

In 2021, rice was produced on $^{\sim}$ 1.1 million ha in the US, and Arkansas was the lead rice-producing state in the US, with $^{\sim}$ 47% of all US rice production [8]. Approximately 76% of all rice grown in Arkansas is flood-irrigated, with the other 24% being irrigated through furrow-irrigation (20%) and intermittent-flooding (4%) schemes [8]. The use of alternative irrigation practices, such as furrow-irrigation, have steadily increased in popularity due to the decreased water-use and equipment and labor costs, resulting in monetary savings for producers [8,9]. Furrow-irrigated rice has shown an overall reduction in water usage up to 48%, resulting in furrow-irrigation receiving increased attention from producers, especially regarding agronomic recommendations and best management practices [10].

Flood-irrigated rice is characterized by large $\mathrm{CH_4}$ emissions due to the constant anaerobic conditions that enhance the process of methanogenesis, and low $\mathrm{N_2O}$ emissions due to the reduced rate of nitrification in anaerobic conditions that

limits the production of substrate necessary for denitrification [11-13]. In contrast, when furrow-irrigation is established, the soil environment is generally aerobic throughout much of the growing season with variation mainly observed along the predominant slope of the fields [14-16]. The aerobic field conditions can result in a significant reduction of CH, and N₂O, as anaerobic processes, such as methanogenesis and denitrification, are restricted. However, soil conditions in furrow-irrigated fields may alternate between aerobic and anaerobic conditions, especially in the mid- and down-slope portions of the field where water can collect, promoting CH, and N₂O production at various points throughout the growing season [14,15]. Consequently, furrow-irrigated rice has the potential to decrease both water usage and GHG emissions compared to flood-irrigated rice, but, if soil moisture and nutrients, especially N, are not properly managed, the potential for N loss via N₃O can be large [13-15]. Furthermore, wet and dry cycles typical of furrow-irrigated rice require tailored agronomic practices for soil fertility and nutrient management substantially different from the ones developed and established in rice under flooded conditions.

Compared to flood-irrigated rice, P management presents a different challenge in furrow-irrigated rice. Typically, the presence of a flood would greatly increase available P in the soil by establishing reducing conditions, freeing P precipitated with iron, but, due to the lack of a flood, P can be a limiting nutrient under furrow-irrigation, as soil P persists in precipitated complexes that are unavailable for plant uptake [17]. Additionally, the application of common fertilizer-P sources to furrow-irrigated rice systems, such as monoammonium phosphate (MAP) and triple superphosphate (TSP), which are highly water soluble, have the potential for P loss by runoff, erosion, and/or soil fixation that pose an additional threat to optimal plant productivity [18,19]. The challenging P management in furrow-irrigated rice thus requires the evaluation of alternative fertilizer-P sources characterized by chemical and physical properties best suited for the dynamic environmental conditions of furrow-irrigated rice fields.

Struvite (MgNH₄PO₄·6H₂O) is a crystalline mineral containing equal molar concentrations of Mg, NH₄, and PO, and is described as a slow-release fertilizer due to the characteristically large weak-acid solubility (i.e., 96% citrate solubility) and low water solubility (i.e., 4%) [20,21]. In addition to supplementing finite RP supply, struvite production could reduce nutrient contamination by both removing N and P from wastewater sources, a portion of which would otherwise be discharged back into the environment and reduce the loss of nutrients in runoff due to the lower water solubility compared to more water-soluble fertilizer-P sources. Previous studies in both field and greenhouse environments of both electrochemically and chemically precipitated struvite have reported that struvite has the potential to serve as an efficient, alternative fertilizer-P source for the production of various crops [22-26] and can reduce the overall global warming potential (GWP) of both flood- and furrow-irrigated rice compared to other common fertilizer-P sources, such as MAP and TSP [27, 28].

Presently, there is a lack of research regarding struvite as a fertilizer-P source in furrow-irrigated rice production and particularly the effects of real-wastewater-derived ECST ($\mathrm{ECST}_{\mathrm{Real}}$) and synthetic ECST ($\mathrm{ECST}_{\mathrm{Syn}}$) on GHG fluxes, emissions and GWP. Thus, the objective of this study was to evaluate the effects of fertilizer-P source [i.e., $ECST_{Real'}$ ECST_{Syn}, chemically precipitated struvite (CPST), MAP, and an unamended control (UC)] on CO₂, CH₄, and N₂O fluxes, season-long emissions, and total and CO, excluded GWPs from simulated furrow-irrigated rice grown in a P-deficient silt-loam soil in the greenhouse. It was hypothesized that peak CH₄, N₂O, and CO₂ fluxes would occur earliest and be greatest for MAP-fertilized rice, followed by ECST_{sun} and ECST_{Real}, CPST, and then the UC due to differences in solubility and fertilizer particle size among the fertilizer-P sources [23,29,30]. Furthermore, it was hypothesized that season-long CH, and CO₂ emissions, total GWP and the CO₂ excluded GWP would not differ among MAP, CPST, ECST $_{\rm Syn}$, and ECST $_{\rm Real}$, but would differ and be smallest from the UC, as the fertilized treatments received the same quantity of nutrients, while UC did not receive any P addition. Season-long N₂O emissions were hypothesized to be greatest from the UC and different from all other fertilizer-P treatments due to the potential stunted plant growth in the UC treatment resulting in limited plant-N uptake and an increased substrate for denitrification. It was also hypothesized that CH_a, N₂O, and CO₂ fluxes, season-long emissions, and total and CO₂ excluded GWPs would not differ between the two ECST fertilizer-P sources, due to the similar physical and chemical properties.

Materials and Methods

Soil collection, processing, and analyses

Approximately 380 kg of low soil-test-P, Calhoun silt-loam (fine-silty, mixed, active, thermic Typic Glossaqualf) soil were collected from the upper 10 to 15 cm of an agricultural field border on 3 December 2022, near Colt, AR at the University of Arkansas, Division of Agriculture's Pine Tree Research Station [31]. The soil-test P concentration at the collection area was intentionally lowered for several years through winter wheat cultivation with no fertilizer-P additions. Soil was sieved through a 6.35 mm mesh screen to remove plant material, coarse fragments, and homogenize the collected soil and was then air-dried at ~ 31°C for one week.

Six sub-samples of air-dried, sieved soil (~ 200 g) were collected for chemical and physical property characterization. Soil sub-samples were weighed, oven-dried at 70°C for a minimum of 48 hours, re-weighed to calculate the initial gravimetric water content (GWC), and sieved through a 2 mm mesh screen. Particle-size analyses were performed using a modified 12-h hydrometer method [32]. The six soil sub-samples were analyzed for soil pH, electrical conductivity (EC), Mehlich-3 (M3) extractable nutrient, total nitrogen (TN), total carbon (TC), and soil OM concentration analyses. A 1:2 soil mass: water volume suspension was used to potentiometrically measure soil EC and pH. Mehlich-3 extractions were conducted in a 1:10 soil mass: extractant volume suspension to quantify extractable soil nutrient (i.e.,

P, K, Ca, Mg, S, Na, Fe, Mn, Zn, Cu, and B) concentrations using inductively coupled, argon-plasma spectrophotometry (ICAPS) [33]. Total C and TN concentrations were determined by high-temperature combustion (VarioMax CN Analyzer, Elementar Americas Inc., Ronkonkoma, NY) and were used to determine the soil C: N ratio [34]. Soil OM was determined by weight-loss-on-ignition in a muffle furnace at 360°C for 2 h [34]. Due to collected soil lacking effervescence when treated with dilute hydrochloric acid, all measured soil C was considered organic C. Soil bulk density was estimated during soil tub preparation (described below) based on the oven-dry mass of soil (~ 22,646 g) within soil tubs divided by the average volume of soil in each tub (~ 19,866 cm⁻³) based on the equivalent volume of water. Initial soil properties are summarized on Table 1.

Treatments and experimental design

A randomized complete block design consisting of five fertilizer-P treatments was evaluated on a single greenhouse bench. Fertilizer-P treatments included MAP, CPST, ECST derived from a synthetic (Syn) solution containing known concentrations of P and N (ECST $_{\rm Syn}$), ECST derived from a local municipal wastewater source (ECST $_{\rm Real}$), and an unamended control (UC) that received no fertilizer-P addition. Fertilizer-P treatments were grouped together into three blocks, each containing one fertilizer-P treatment, for a total of 15 experimental units (i.e., tubs).

Fertilizer-P sources and characterization

Monoammonium phosphate (fertilizer grade: 11-52-0) represents a widely used and commercially available

Table 1: Summary of mean [± standard error (SE)] initial properties of the Calhoun silt-loam soil used in the greenhouse study in 2023 (n = 6).

| Soil property | Mean (± SE) |
|---|----------------|
| Sand (g g ⁻¹) | 0.14 (0.00) |
| Silt (g g ⁻¹) | 0.72 (0.01) |
| Clay (g g ⁻¹) | 0.14 (0.01) |
| Bulk density (g cm ⁻³) | 1.14 (< 0.01) |
| pH | 7.4 (0.05) |
| Electrical conductivity (dS m ⁻¹) | 0.268 (0.01) |
| Extractable soil nutrients (mg kg ⁻¹) | |
| Phosphorus | 10.5 (0.2) |
| Potassium | 80.96 (1.6) |
| Calcium | 1559.10 (26.3) |
| Magnesium | 224.10 (3.2) |
| Sulfur | 11.37 (0.3) |
| Sodium | 60.28 (1.3) |
| Iron | 218.87 (5.0) |
| Manganese | 257.60 (25.4) |
| Zinc | 7.0 (0.1) |
| Copper | 1.24 (0.05) |
| Boron | 0.19 (0.01) |
| Soil organic matter (g kg ⁻¹) | 15.7 (0.08) |
| Total carbon (g kg ⁻¹) | 5.05 (0.01) |
| Total nitrogen (g kg ⁻¹) | 0.59 (< 0.01) |
| Carbon : nitrogen ratio | 8.59 (0.1) |

Table 2: Summary of fertilizer-phosphorus (P)-source fertilizer grade and mean pH and nutrient concentrations [± standard error (SE)] and water solubility.

| Fertilizer-P | Measured | | Nutrient con | centration (± S | Fertilizer-P source water | |
|----------------------|----------------------------------|-------------|--------------|-----------------|---------------------------|-------------------------|
| source ^a | fertilizer grade ^b | рН | N | P | Mg | solubility ^d |
| | | | | % | | |
| ECST _{Real} | 3-35-0 | 7.2 (< 0.1) | 3.3 (0.1) | 15.5 (0.2) | 13.6 (0.3) | 2 - 3.8% |
| ECST _{Svn} | 5-37-0 | _c | 5.1 (0.2) | 16.1 (0.3) | 12.7 (0.3) | 2 - 3.8% |
| MAP | 11-52-0 | 4.4 (0.02) | 10.7 (0.1) | 22.7 (0.2) | 1.5 (< 0.1) | 85 - 90% |
| CPST | 6-27-0 | 8.8 (0.13) | 5.7 (0.2) | 11.7 (0.2) | 8.3 (0.2) | 4% |

^a Electrochemically-precipitated synthetic struvite (ECST_{Syn}), wastewater derived electrochemically-precipitated struvite (ECST_{Real}), monoammonium phosphate (MAP), and chemically-precipitated struvite (CPST).

fertilizer-P source for rice production [35]. Although other fertilizer-P sources, such as TSP (fertilizer grade: 0-46-0) and diammonium phosphate (fertilizer grade: 18-46-0) are more commonly used in Arkansas agriculture, MAP was chosen due to the similarities in fertilizer grade with the other struvite-P sources that were used in this study (fertilizer grade: 6-27-0 for CPST, 5-37-0 for ECST $_{\rm Syn}$, and 3-36-0 for ECST $_{\rm Real}$; Table 2) [35]. Monoammonium-phosphate-treated experimental units received fertilizer in the commercially available, pelletized form. Compared to the other fertilizer-P sources that were evaluated by this study, MAP was the most water-soluble (85 to 90%) [29].

Crystal Green, a CPST produced by Ostara Nutrient Recovery Technologies, Inc. (Vancouver, Canada), was used in this study as the CPST fertilizer-P source in the commercially available, pelletized form. Commercially available Crystal Green pellets ranged in size from 2.5 to 3 mm in diameter. Ostara [36] reported Crystal Green solubilities of 4 and 96% in water and citrate, respectively (Table 2) [23]. The CPST fertilizer-P source contained ~ 8.3% magnesium (Mg) [23].

Electrochemical precipitation was used to precipitate the $\mathrm{ECST}_{\mathrm{Real}}$ and $\mathrm{ECST}_{\mathrm{Syn}}$ materials out of solution using a Mg anode as a sacrificial Mg source [37]. A synthetic solution of known P and N concentration, in the form of phosphate and ammonium (NH,+), was prepared at the University of Arkansas' Department of Chemical Engineering to produce the ECST_{svn} fertilizer material [37]. A wastewater sample was collected from the West Side Wastewater Treatment Facility in Fayetteville, AR to serve as the substrate from which the $\mathrm{ECST}_{\mathrm{Real}}$ material was produced using the same electrochemical process as the ECST_{Svn} material. The struvite materials produced from electrochemical precipitation were crushed into powder from the original crystalline structure for chemical analysis of N, P, K, and Mg concentrations and pH. As detailed by USEPA [38], a nitric acid digest was used to measure total-recoverable N, P, K, and Mg concentrations using ICAPS [23]. A 1:2 fertilizer mass: water volume paste was created to potentiometrically measure the pH of the ECST material. Overall water solubility was lowest for the ECST fertilizer-P sources compared to the other fertilizer-P sources (2 to 3.8%) [30]. Initial chemical properties for each fertilizer are summarized in Table 2.

Soil tub preparation

Plastic soil tubs (55.5 cm long by 39.1 cm wide by 15.1 cm tall, interior dimensions) were filled with $^{\sim}$ 24 kg of airdried, sieved soil and placed onto a single greenhouse bench (1.2 m wide by 4.9 m long and 1.1 m tall) to provide a level bench top for the duration of the greenhouse study. Polyvinyl chloride (PVC) base collars (3 cm diameter by 2.54 cm thick by 30 cm tall) with four, equidistant 1 cm diameter drilled holes15 cm from the bottom were pushed into the soil to the bottom of each plastic tub to serve as the foundation for GHG measurement caps and extensions (described below) and to facilitate the movement of surface water between the areas inside and outside the base collars. After base collars were installed, the soil was saturated, left to settle, and the distance from the top of the tub to the soil surface was recorded on all four sides of each soil tub. The average height of the soil was used to determine the volume of the soil mass in the soil tubs using an equivalent height of water. The average height of soil was marked on three empty tubs and the volume of water required reaching that height was recorded as the estimated average volume of settled soil in the tubs and used to estimate the soil bulk density.

Rice establishment and fertilization

Soil tubs were watered until visibly wet, twice a week with three days between watering to promote weed growth. Weeds were removed twice a week, until rice was planted, to eliminate any effect on soil fertility. The hybrid rice variety RT 7302 (RiceTec) was seeded manually into visibly wet soil to a depth of ~ 2 cm on 16 April 2023 at a rate of 124 seeds m⁻² for a total of 27 seeds per tub. Rice was planted into three parallel rows of 9 seeds along the long side of the soil tubs. Rows were planted 15.6 cm apart, with 5.9 cm of space between seeds in a row. Approximately 4 cm of soil was reserved from the border on each side of the soil tubs to minimize the effect of limited soil availability to the rice plants closest to the tub borders. After rice was planted, weeds were removed manually throughout the season to eliminate weed pressure on rice plants. Rice plants in each tub were culled seven days after P, K, and Zn fertilizers were applied to have four rice plants within the collar and 10 rice plants outside the collar for a total of 14 present in each soil tub to reach the

^b Measured fertilizer grade expressed as % N - P₂O₅ - K₂O.

 $^{^{\}rm c}\textsc{Limited}\ \textsc{ECST}_{\textsc{syn}}$ supply prohibited pH determination.

^dFertilizer characteristic not determined through lab analysis.

optimum stand density for hybrid-variety rice of 65 to 108 plants m^{-2} [13,35,39].

Based on initial soil chemical properties, N, P, and K fertilizers were applied to the experimental tubs based on recommendations from the Arkansas Rice Production Handbook [35], the Arkansas Furrow-irrigated Rice Production Handbook [16], and the Arkansas Rice Management Guide [40] for the RT 7302 hybrid rice variety grown in a silt-loam soil. Based on Bouman and Tuong [41], Craswell and Vlek [42], and Slayden, et al. [13], fertilizer recommendations were increased by 20% to minimize negative effects of limited soil volume on nutrient availability. Fertilizer-P, -K, and -Zn sources were applied to the soil surface of each soil tub immediately after planting [16]. Phosphorus, K and Zn were applied at rates of 35.2 kg P ha⁻¹, 100.5 kg K ha⁻¹, and 5.5 kg Zn ha⁻¹, respectively [35]. A total of 17.1 kg ha⁻¹ of N in the form of N-(n-butyl) thiophosphoric triamide (NBPT)-coated urea (46% N) was added to both ECST sources, CPST, and the UC to equalize the amount of N applied to each tub during the P, K, and Zn fertilizer application to match the supply of N from MAP. Muriate of potash and zinc sulfate were applied as the fertilizer-K, and -Zn sources. After P, K, and Zn fertilizers were manually broadcast onto the soil surface, each tub was irrigated to 52% volumetric water content (VWC) using filtered tap water to incorporate nutrients into the soil.

Nitrogen was applied to soil in a four-way split throughout the beginning of the growing season. Prior to N fertilizations, no water was added for two days to allow the soil surface to dry to minimize N loss via ammonia volatilization after urea applications. Nitrogen applied during P fertilization was subtracted from the first recommended fertilizer-N application to achieve the recommended initial application amount [35]. Nitrogen was applied 29, 36, 43, and 78 days after planting (DAP) at a rate of 50.2, 67.3, 67.3, and 26.9 kg N ha⁻¹, respectively, for a total of 228.7 kg N ha⁻¹ [16,40]. Filtered tap water was used to immediately irrigate the soil to 52% VWC to incorporate N fertilizer after each fertilizer-N application.

Water management

Soil moisture sensors (200SS WaterMark Sensor, Irrometer Inc., Riverside, CA) were installed into six soil tubs, two from each block of the same fertilizer-P treatments, 10 DAP to a depth of 7.6 cm. Sensors were connected to a central data logger that was manually checked every three days from 10 DAP until 50 DAP and every two days thereafter until the end of the growing season due to increased greenhouse air temperatures. From 10 to 160 DAP, when a soil matric potential less than or equal to -10 kPa was recorded, soil tubs were irrigated to a uniform, near-saturated, target VWC (i.e., ~ 52%). The near-saturated VWC target was based on previous studies conducted by Slayden, et al. [13] and Della Lunga, et al. [14,28] to minimize N₃O production.

Prior to water additions, a soil moisture probe (SM 150, Delta-T Devices Ltd., Cambridge, UK) was used to measure the soil VWC in the top 6 cm inside and outside of the base collar in each tub and were averaged to determine the current

VWC. Average VWC measurements less than the target VWC had the amount of water equal to the difference between the target and current VWC added using filtered tap water. After planting, but prior to sensor installation, soil VWC was measured every two days and water was added to reach the near-saturation VWC target. Filtered water was used throughout this study to eliminate the potential effect of elevated salts known to be present in the tap water available in the greenhouse. The final watering event occurred 160 DAP to allow soil tubs to fully dry before harvesting at 170 DAP [35].

Gas sample collection, analyses, and calculations

Gas sampling occurred weekly over a continuous period of 23 weeks, beginning 3 DAP on 19 April 2023 and ending 162 DAP on 25 September 2023. Gas sampling took place between 0800 and 1000 hours on each of the 24 measurement dates (i.e., 3, 9, 16, 22, 29, 36, 43, 50, 57, 64, 71, 78, 85, 92, 99, 106, 113, 120, 127, 134, 141, 148, 155, and 162 DAP) similar to recent greenhouse studies [13,28]. Polyvinyl chloride (PVC) caps (30 cm in diameter by 10 cm tall) were placed onto the base collars and sealed using a rubber flap along the seam and four 1.3 cm diameter rubber stoppers to plug the four holes in each base collar. The interior sidewall of each chamber cap was installed with a 15 cm long copper refrigerator tube with an interior diameter of 0.63 cm to equilibrate interior and exterior pressures. Chamber-cap interiors were also mounted with a 2.5 cm² fan wired to a 9 V battery to mix air within the closed chamber throughout each sampling. Additionally, caps were fitted with a 1.3 cm diameter rubber septum to maintain closed-chamber integrity during the collection of gas samples using a 20 mL syringe. A second 1.3 cm diameter septum was installed into a single chamber cap to allow the insertion of a thermometer to measure the inside-chamber air temperature during the gas sampling period. Chamber extensions, 40- or 60-cm tall and 30 cm in diameter, were used as needed throughout the growing season to account for the increasing height of growing plants and were connected along the seam using a rubber flap.

Gas samples were collected from the closed chambers at 0, 30, and 60 minute time intervals relative to cap mounting and sealing, for a total of 45 gas samples per sample date [13,42]. A 20 mL syringe with a 25 mm long, 0.5 mm-diameter needle was used to collect 20 mL of headspace gas from each closed chamber at the three time intervals by puncturing the cap septum, with separate syringes used between chambers to prevent contamination. Syringes were slowly aspirated to allow collected headspace gas to fully mix within the syringe before being immediately transferred into a preevacuated, 10 mL, glass vial with pre-crimped steel cap (20 mm headspace crimp cap). The height of the headspace in each chamber was measured during each sampling from the soil surface to the top of the chamber lid to properly calculate the chamber volume. Throughout the growing season, a portable weather station (AcuRite, Schaumburg, IL) was used to record the greenhouse air temperature, barometric pressure, and relative humidity at the 0, 30, and 60 min sampling intervals within the 0800- to 1000-h sampling period for each gas sampling event. Additionally, the chamber's internal air temperature was recorded at the 0-, 30-, and 60-min time intervals using a thermometer inserted through one chamber's extra cap septa.

A Shimadzu GC-2014 ATFSPL 115-V gas chromatograph (GC; Shimadzu North America/Shimadzu Scientific Instruments Inc., Columbia, MD) was used for gas sample analyses within 24-h of collection. A total of 59 gas samples were analyzed following each gas sampling date. The additional 14 gas samples included standards that consisted of five samples with increasing CH₄ concentrations (i.e., 1, 5, 10, 20, and 50 mg kg $^{-1}$), six samples with increasing N $_2$ O concentrations (i.e., 0.1, 0.5, 1, 5, 10, and 20 mg kg⁻¹), and three samples with increasing CO₂ concentrations (i.e., 300, 500, and 1000 mg kg⁻¹). Nitrous oxide concentrations were measured using an electron-capture detector (ECD) while a flame-ionization detector (FID) coupled with a methanizer was used to measure CH₄ and CO₂ concentrations. Gas fluxes across the 1-h measurement period (mg m⁻² h⁻¹) were calculated using the best fit of a linear regression by multiplying the chamber volume by the slope of the linear regression among the measured gas concentrations across the three gas sampling time intervals [11-14, 43-47]. A value of zero was reported for gas fluxes with negative linear regression slopes to remove GHG uptakes and only report emissions. Gas fluxes were interpolated between consecutive measurement dates, on a chamber-by-chamber basis, to determine season-long emissions (kg ha⁻¹ season⁻¹).

In addition to gas fluxes and season-long emissions, total and $\rm CO_2$ -excluded GWPs were calculated using the 100-yr conversion factors from the 6th IPCC report for each fertilizer-P treatment [2,48]. The total GWP was calculated as the sum of season-long $\rm CH_4$ and $\rm N_2O$ $\rm CO_2$ equilvalents and season-long $\rm CO_2$ emissions. The $\rm CO_2$ excluded GWP was the sum of season-long $\rm CH_4$ and $\rm N_2O$ $\rm CO_2$ equilvalents. The $\rm CO_2$ excluded GWP was calculated due to the difference in magnitude and manageability associated with $\rm CO_2$ compared to $\rm CH_4$ and $\rm N_2O$, as the $\rm CO_2$ magnitude is generally substantially greater and the majority of agricultural GHG reduction studies focus on $\rm CH_4$ and $\rm N_2O$ (49]. The 6th assessment's $\rm CH_4$ and $\rm N_2O$ conversion factors of 28 and 265, respectively, were used to calculate $\rm CO_3$ -equivalents [2,48].

Season-long greenhouse climate data were recorded during each sampling event from 19 April 2023 to 25 September 2023 and were summarized in Table 3. Internal chamber air temperatures throughout the growing season ranged from 21.4 to 37.0°C and averaged 29.6°C (Table 3). Additionally, season-long greenhouse air pressure ranged from 75.5 to 101.41 cm Hg and averaged 76.4 cm Hg (Table 3).

Statistical analyses

A two-factor analysis of variance (ANOVA) was performed as a split-plot experimental design with time as the splitplot factor and fertilizer-P source as the whole-plot factor to evaluate the effects of fertilizer-P treatment, time (i.e., measurement date), and their interaction on CO₂, CH₄, and N₂O gas fluxes. A randomized complete block with three blocks was used as the experimental design for the whole-plot factor. A one-factor ANOVA was performed to evaluate the effect of fertilizer-P treatment on season-long CO₂, CH₄, and N₂O emissions, and total and CO₂-excluded GWPs. Prior to formal statistical analyses, data distributions were checked using JMP Pro (version 17, SAS Institute, Inc., Cary, NC) to determine if a gamma or normal distribution was most appropriate based on Akaike information criteria (AIC). Consequently, a gamma distribution was used for GHG fluxes, while a normal distribution was used for the remaining response variables analyzed. All statistical analyses were conducted in SAS (version 9.4, SAS Institute, Inc., Cary, NC) using the PROC GLIMMIX procedure. Externally studentized residuals were visually evaluated in SAS to assess independence, homoskedasticity and outliers. As result the assumption for generalized mixed models or ANOVA were considered valid and the split-plot design was considered appropriate to characterize the structure of the data. No outlier was identified, and all the datasets were complete and balanced. Significance was determined at P < 0.05. When appropriate, means were separated by least significant difference.

Results

Initial soil properties

Prior to soil tub preparation, initial soil chemical and physical properties were assessed before treatments were applied to the soil used in the current study. Average sand, silt, and clay confirmed a silt-loam soil texture (Table 1). Initial mean soil pH was greater than what is recommended for furrow-irrigated rice production in Arkansas (pH < 7.0), especially in soils with low or very low soil-test-P (< 16 mg kg-1), due to the risk potential for damaging P-deficiency symptoms in the plants [16] (Table 1). Additionally, soil pH was greater than what is considered optimal for Zn (pH < 6.0) in flood-irrigated rice, which, in furrow-irrigated rice, is considered a micronutrient of concern due to the lack of a flood and subtle symptoms that could negatively affect rice yield [16,35]. Potassium fertilizer was applied as muriate of potash due to mean initial soil-test K (81.0 mg kg⁻¹; Table 1) being less than the recommended optimal level for floodirrigated rice production (131-175 mg kg⁻¹) [35]. Mean initial soil-test-Zn (7.0 mg kg-1; Table 1) was greater than the optimal recommended level for flood-irrigated rice (> 4.1 mg kg⁻¹), but,

Table 3: Summary of season-long average, maximum, and minimum greenhouse climate conditions during the 2023 greenhouse study.

| Descriptive statistic | Air temperature (C°) | Chamber air temperature (C°) | Greenhouse pressure (cm Hg) | Relative humidity (%) |
|-----------------------|----------------------|------------------------------|-----------------------------|-----------------------|
| Mean | 27.9 | 29.6 | 76.4 | 54.8 |
| Maximum | 32.0 | 37.0 | 101.4 | 85.0 |
| Minimum | 21.0 | 21.4 | 75.5 | 20.0 |

due to the risk for subtle Zn deficiency symptoms in furrowirrigated rice, Zn fertilizer was applied to avoid any potential issue [16,35]. The mean initial soil-test P (10.5 mg kg⁻¹; Table 1) was low (9-16 mg kg⁻¹) for a soil with a pH greater than or equal to 6.5 [35]. Additionally, the relatively low C:N ratio (1:8.59) indicates that N mineralization is favored and likely facilitated the release of inorganic N from the organic N pool. Due to the initial low soil-test-P, a rice plant response was expected with fertilizer-P addition.

Greenhouse gas fluxes

Methane, N_2O , and CO_2 fluxes varied widely temporally among fertilizer-P treatments throughout the growing season and differed (P < 0.05) among fertilizer-P sources over time

(Table 4). Methane fluxes ranged from < 0.01 mg CH $_4$ m $^{-2}$ h $^{-1}$ from ECST $_{\rm Real}$ at 29 DAP to 0.15 mg CH $_4$ m $^{-2}$ h $^{-1}$ at 120 DAP from CPST (Figure 1A). As was expected for a non-flooded system, CH $_4$ was minimal throughout the growing season, with only four measurements numerically greater than 0.1 mg CH $_4$ m $^{-2}$ h $^{-1}$, three of which occurred at 113 DAP (Figure 1A). Additionally, throughout the growing season, 90% of all CH $_4$ flux measurements recorded were less than 0.05 mg CH $_4$ m $^{-2}$ h $^{-1}$ (Figure 1A). Throughout the 24 total sampling events, CH $_4$ flux measurements did not differ (P > 0.05) from a flux of zero on eight sample dates for any of the fertilizer-P sources (i.e., 9, 16, 36, 78, 106, 127, 148, and 155 DAP). Furthermore, CH $_4$ flux measurements differed (P < 0.05) among fertilizer-P treatments on 13 of the 24 sampling dates (i.e., 3, 22, 29, 43,

Table 4: Analysis of variance summary of the effects of fertilizer-phosphorus (P) source, days after planting (DAP), and their interaction on methane (CH_4) , carbon dioxide (CO_2) , and nitrous oxide (N_2O) fluxes during 2023 in the greenhouse.

| Descriptive statistic | Air temperature (C°) | Chamber air temperature (C°) | Greenhouse pressure (cm Hg) | Relative humidity (%) |
|-----------------------|----------------------|------------------------------|-----------------------------|-----------------------|
| Mean | 27.9 | 29.6 | 76.4 | 54.8 |
| Maximum | 32.0 | 37.0 | 101.4 | 85.0 |
| Minimum | 21.0 | 21.4 | 75.5 | 20.0 |

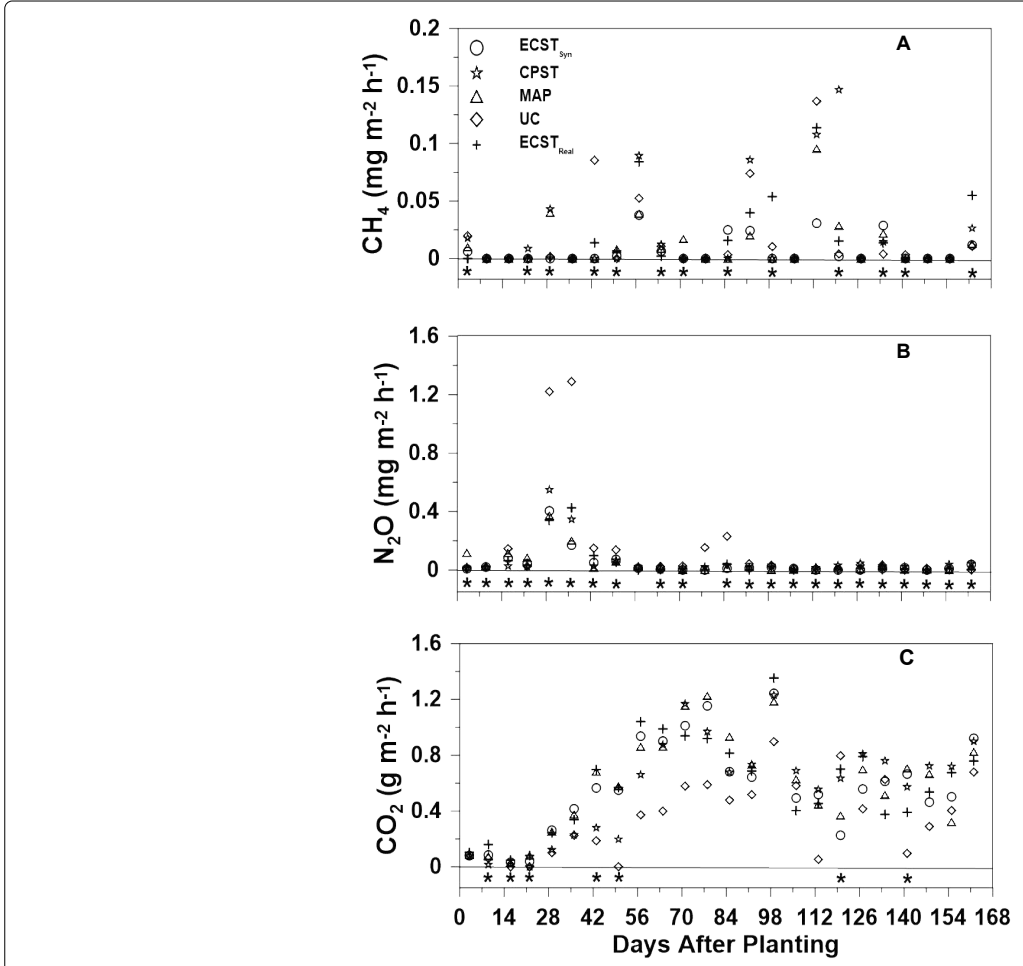


Figure 1: Methane (CH₄), nitrous oxide (N₂O), and carbon dioxide (CO₂) fluxes for five fertilizer-phosphorus (P) treatments [i.e., real-wastewater-derived (ECST_{Real}) and synthetic-solution-derived electrochemically precipitated struvite (ECST_{Syn}), chemically precipitated struvite (CPST), monoammonium phosphate (MAP), and a no-fertilizer-P, unamended control (UC)] from furrow-irrigated rice in the greenhouse. Asterisks (') represent days in which CH₄, N₂O, and CO₂ fluxes differed (P < 0.05) among fertilizer-P sources. Fertilizer-P, -K, and -Zn sources were applied at planting and fertilizer-N additions occurred 29, 36, 43, and 78 days after planting.

Table 5: Summary of the effects of fertilizer-phosphorus (P) source on season-long methane (CH_4), nitrous oxide (N_2O), and carbon dioxide (CO_2) emissions, and total global warming potential (GWP) and CO_2 -excluded GWP using the IPCC sixth (IPCC, 2021) assessment conversion factors during 2023 in the greenhouse.

| Greenhouse gas property | 5 | Fertilizer-P source | | | | | Overall |
|---|----------------------------|--------------------------------------|----------------------------------|-------------------|---------|-----------------|---------|
| | P | ECST _{Real} a | ECST _{Svn} ^a | CPST ^a | MAPa | UC ^a | mean |
| Season-long Emissior | าร | | ., | | | | |
| CH ₄ (kg ha ⁻¹) | 0.28 | 0.65 | 0.26 | 0.88 | 0.47 | 0.67 | 0.59 |
| N ₂ O (kg ha ⁻¹) | < 0.01 | 1.9 b* | 1.6 b | 2.2 b | 1.8 b | 6.1 a | - |
| CO ₂ (Mg ha ⁻¹) | 0.01 | 23.0 a | 22.0 a | 22.0 a | 23.3 a | 13.6 b | - |
| Total GWP (kg CO ₂ -e | quivalents ha | ⁻¹ season ⁻¹) | | | · | · | · |
| | 0.02 | 23487 a | 22458 a | 22655 a | 23819 a | 15215 b | - |
| CO ₂ -excluded GWP (I | kg CO ₂ -equiva | alents ha-1 seaso | on ⁻¹) | | | | |
| | < 0.01 | 530.3 b | 425.1 b | 608.7 b | 488.0 b | 1622.7 a | - |

^a Electrochemically precipitated struvite made from a synthetic solution, ECST_{Syn}; electrochemically precipitated struvite made from a real wastewater, ECST_{Real}; chemically precipitated struvite, CPST; monoammonium phosphate, MAP; unamended control, UC ^{*} Means followed by a letter with the same case do not differ (P > 0.05)

50, 64, 71, 85, 99, 120, 134, 141, and 162 DAP). In contrast to that hypothesized, the CH $_4$ flux peak occurred at 120 DAP for CPST, which differed (P < 0.05) from all other fertilizer-P treatments on that sampling date (Figure 1A). Additionally, peak CH $_4$ fluxes occurred at 57 DAP for ECST $_{\rm Real}$, MAP, and the UC, in which CH $_4$ fluxes did not differ among fertilizer-P sources at either 57 or 113 DAP (Figure 1A). In contrast to that hypothesized, ECST $_{\rm Syn}$ and ECST $_{\rm Real}$ differed (P < 0.05) for CH $_4$ during 5 of the 24 sampling dates (i.e., 3, 29, 43, 99, and 120 DAP; Figure 1A).

Similar to CH₄, N₂O fluxes were generally low and ranged from < 0.01 mg N₂O m⁻² h⁻¹ at 99 DAP from MAP to 1.29 mg $N_{\gamma}O$ m⁻² h⁻¹ at 36 DAP from the UC (Figure 1B). However, in contrast to CH, fluxes, NO fluxes were greatest during the early growing season when the majority of fertilizer-N was applied, peaked at 36 DAP from the UC, and then largely remained low (< 0.2 mg N₂O m⁻² h⁻¹) for the remainder of the growing season, with the exception of one N₂O flux at 85 DAP from??? (Figure 1B). Throughout the growing season, N₂O fluxes differed (P < 0.05) among fertilizer-P sources on 22 of the 24 total sampling dates, except for at 57 and 78 DAP (Figure 1B). Additionally, N,O fluxes did not differ (P > 0.05) from zero for all fertilizer-P treatments on 2 of the 24 sampling dates (i.e., 29 and 36 DAP; Figure 1B). Although the numeric peak N₂O flux occurred at 36 DAP for the UC, the flux did not differ from a flux of zero, as large variability among replicates resulted in wide confidence intervals that included zero (Figure 1B). As was hypothesized, N₂O fluxes from both ECST fertilizer-P sources were similar (P > 0.05) during each of the 24 sample dates.

As expected, CO_2 fluxes throughout the growing season were orders of magnitude greater than for CH_4 and N_2O_7 , ranging from 0.01 g CO_2 m⁻² h⁻¹ at 16 DAP from CPST to 1.4 g CO_2 m⁻² h⁻¹ at 99 DAP from ECST_{Real} (Figure 1C). Generally, CO_2 fluxes began relatively low (< 0.3 g CO_2 m⁻² h⁻¹) and steadily increased with plant growth, beginning ~ 29 DAP, peaking at 99 DAP, and then decreasing to a near-constant level for the remainder of the growing season, with 84% of CO_2 fluxes occurring from 106 to 162 DAP being between 0.4 and 0.8

g CO₂ m⁻² h⁻¹ (Figure 1C). Carbon dioxide fluxes differed (P < 0.05) from zero in all instances, except on four measurement dates at 16, 22, and 50 DAP for the UC and at 22 DAP for CPST (Figure 1C). Generally, CO_3 fluxes were similar (P > 0.05) among fertilizer-P treatments and only differed (P < 0.05) among fertilizer-P treatments on seven of the 24 sampling dates (i.e., 9, 16, 22, 43, 50, 120, and 141 DAP). Similar to that hypothesized, numeric peak CO, fluxes occurred earliest for MAP at 78 DAP and at 99 DAP for CPST, ECST_{Syn}, ECST_{Real}, and the UC, but, in contrast to that hypothesized, did not differ (P > 0.05) from one another, thus no clear pattern for CO₃ fluxes based on fertilizer-P sources was identified based on the temporal flux trends. Carbon dioxide fluxes did not differ between the two ECST fertilizer-P sources on 23 of the 24 gas sampling dates but differed from each other at 120 DAP (Figure 1C).

Season-long emissions

Season-long $\mathrm{CH_4}$, $\mathrm{N_2O}$, and $\mathrm{CO_2}$ emissions were determined to represent the cumulative release of GHG most relevant to rice production systems in Arkansas. Due to protocol procedures, season-long emissions are to be considered an over-estimation of the actual GHG input into the atmosphere as no sink process was considered in the current study. Season-long $\mathrm{N_2O}$ emissions were at least 2.8 times greater from the UC compared to CPST, MAP, and both of the ECST-P sources (Table 5). Season-long $\mathrm{CO_2}$ emissions were at least 1.6 times greater from $\mathrm{ECST}_{\mathrm{Real}}$, $\mathrm{ECST}_{\mathrm{Syn}}$, CPST, and MAP compared to the UC (Table 5). As was hypothesized, the $\mathrm{ECST}_{\mathrm{Syn}}$ and $\mathrm{ECST}_{\mathrm{Real}}$ did not differ (P > 0.05) from one another for season-long $\mathrm{CH_4}$, $\mathrm{N_2O}$, and $\mathrm{CO_2}$ emissions (Table 5).

Global warming potential

Total GWP and CO_2 excluded GWP were calculated using conversion factors from the 6th IPCC assessment to integrate the combined effect of each GHG and, regarding the CO_2 -exluded GWPs, to provide a CH_4 and $\mathrm{N}_2\mathrm{O}$ focused analysis of GWP. Furthermore, the CO_2 excluded GWP was calculated because the much greater magnitude of CO_2 emissions can mask potential differences in GWP among fertilizer-P sources

associated with ${\rm CH_4}$ and ${\rm N_2O}$ [27]. Total GWP for the P-fertilized treatments was at least 1.5 times greater compared to the UC (Table 5). The ${\rm CO_2}$ -excluded GWP from the UC was at least 2.7 times greater compared to the treatments that received fertilizer-P applications (Table 5).

Discussion

Analysis of GHG fluxescan improves the sustainability of furrow-irrigated rice production by determining critical periods when GHG emissions occur and help guide management practices to mitigate those emission events. As noted by previous studies in both greenhouse and field settings, methanogenesis can be and likely was limited by the lack of saturated soil and reducing conditions and was likely a major controlling factor influencing CH, fluxes in the current study [27,28]. Della Lunga, et al. [27] reported CH fluxes from a similar simulated furrow-irrigated rice study in the greenhouse that were temporally similar to the current study, as a numerically largest peak CH, flux of 0.21 mg CH, $m^{\text{--}2}\ h^{\text{--}1}$ occurred at 91 DAP for the ECST $_{\text{Syn}}$ fertilizer-P source compared to the largest $\mathrm{CH_4}$ peak at 120 DAP from CPST, a similar struvite fertilizer-P source, in the current study. In contrast, the magnitude of CH, fluxes reported in the current study were at least half of the flux values reported by Della Lunga, et al. [28], another similar simulated furrow-irrigated rice system on a silt-loam soil in the greenhouse. Additionally, CH₄flux comparisons throughout the season largely emphasized the comparability of the two ECST fertilizer-P sources. Although the ECST-P sources were similar in chemical composition and particle size, variation in soil moisture and plant response, as documented by Arel, et al. [50], could have resulted in differences in dissolution in the soil that would have stimulated anaerobic pockets in the rhizosphere where methanogenesis occurred [50,51]. However, differences between ECST-P sources had no discernible pattern during the growing season.

Season-long analysis of $\rm N_2O$ fluxes generally reported similar trends and values for P-receiving treatments, with the UC reporting the greatest potential for N loss via denitrification as the numerically greatest peaks occurred from the UC following N fertilization (Figure 1B). The flux peak likely occurred for the UC as a result of the sub-optimal P fertilization that resulted in stunted pant growth, a decreased N uptake and allowed a greater soil-N concentration to remain and be susceptible to nitrification and subsequent denitrification.

Compared to N_2O fluxes from furrow-irrigated rice production reported previously from greenhouse and field settings, the current study was often comparable in trend, but smaller in magnitude. Previous greenhouse studies reported peak N_2O fluxes of 2.3 mg N_2O m⁻² h⁻¹ at 63 DAP [13] and 2.2 mg N_2O m⁻² h⁻¹ at 31 DAP [28] from optimally fertilized treatments. At the field scale, Slayden, et al. [46] reported N_2O fluxes over a 2-year study period that were much greater in magnitude to that reported in the current study, as N_2O flux peaks regularly exceeded 1.0 mg N_2O m⁻² h⁻¹, peaking at 9.7 mg N_2O m⁻² h⁻¹, and emphasized the large variability of N_2O fluxes based on field position within a production-scale,

furrow-irrigated rice field. Additionally, Slayden, et al. [46] reported no consistent temporal pattern for $\rm N_2O$ fluxes, but noted that $\rm N_2O$ flux peaks typically lagged one to two weeks behind fertilizer-N applications. In contrast to Slayden, et al. [46], Della Lunga, et al. [27] reported similar $\rm N_2O$ fluxes to that in the current study, with N₂O fluxes peaking at $^{\sim}$ 0.9 mg N₂O $\rm m^2~h^{-1}$ at 35, 70, and 112 DAP. Although comparable, previous studies and the current study likely differed in nitrification and denitrification potentials, as varying concentrations of $\rm NO_3^-$ from both soil N and nitrifiable ammonium (NH₄+) from applied NBPT-coated urea would have directly impacted the N₂O flux peaks and season-long N₂O emissions, as NO₃- is required for denitrification.

Carbon dioxide fluxes measured in the current study were comparable in both range and temporal trend to that reported in previous greenhouse and field studies [15,27,28,52]. Similar to previous research, CO, fluxes began low early in the growing season and then steadily increased, generally peaking between 80 and 100 DAP, during which rice plants entered reproductive (R) stages (R0 - R9) of their life cycles, followed by a general decline in CO₃ fluxes until plants were harvested [15,27,28,35]. Although smaller in magnitude, CO, flux trends in the current study were similar to a previous greenhouse study [28], in which CO, fluxes peaked at 2.5 g CO₂ m⁻² h⁻¹ at 101 DAP for CPST compared to the current study in which CO₂ fluxes peaked at 1.35 g CO₂ m⁻² h⁻¹ at 99 DAP for $\mathsf{ECST}_\mathsf{Real'}$ which was similar to all other fertilizer-P treatments (Figure 1C). Furthermore, CO₂ fluxes measured in the current study were most similar in magnitude to CO₂ fluxes reported by Della Lunga, et al. [15] at the up-slope field positions, where aerobic conditions prevailed.

The lack of flooded-soil conditions greatly reduced CH, emissions. Furthermore, the range of season-long CH, emissions reported in the current study was similar compared to previous greenhouse and field studies that evaluated the effects of various fertilizer-P sources, including ECST_{sun}, CPST, and an UC [27,28]. Additionally, compared to season-long CH₄ emissions reported by Humphreys, et al. [53], which ranged from 63 to 336 kg CH₄-C ha⁻¹ season⁻¹ from rice grown in flood-irrigated conditions in the field, the current study emphasizes the great potential for CH_4 reduction from furrow-irrigated rice production. Della Lunga, et al. [28] reported that season-long CH, emissions were more than five times greater from a flood-compared to the adjacent furrowirrigated system in the greenhouse. Furthermore, within the furrow-irrigated treatments, grain yield did not differ among fertilizer-P source, but a significant reduction in CH₄ emissions was reported compared to all other fertilizer-P treatments [28]. Similarly, ECST was significantly less than all other fertilizer-P sources and differed (P < 0.05) when converted to an emissions intensity [28]. In contrast to the magnitude of CH₄ emissions reported in the current study, Timms, et al. [54] reported season-long CH₄ emissions of 187, 48, and 72 kg ha⁻¹ from the down-, intermediate-, and up-slope field positions from a paddy rice field in Brazil growing the hybrid rice variety XP 117 (RiceTec, Brazil) during the 2020 to 2021 growing seasons. Although more similar in magnitude to CH, emissions reported by flood-irrigated studies conducted in

the southeastern U.S., Timms, et al. [54] reported an overall reduction of CH, emissions by 61 and 40% in the up- and intermediate-slope positions, respectively, compared to the continuously flooded down-slope position, emphasizing the potential for reductions in CH₄ emissions regardless of the CH₄ production potential across soil with differing physical and chemical properties. Similar in trend to Timms, et al. [54], Karki, et al. [55] reported a 77% reduction in CH₄ emissions from the down- compared to the up-slope field position in a furrow-irrigated Arkansas rice field. Although the magnitude of CH₄ emissions were approximately 1.5 to 5 times greater than that reported in the current study, likely due to the greater initial soil C concentration, where the similar trend in the reduction of CH, production through the use of hybrid rice cultivars in furrow-irrigation systems underscores the potential to reduce GHG emissions. As hypothesized, season-long $CH_{\underline{a}}$ emissions did not differ between $ECST_{Real}$ and ECST_{syn}likely due to similar particle-sizes, dissolution characteristics, and nutrient concentrations (Table 5).

Season-long N₂O emission were likely greatest from the UC because of the lack of available P for plant uptake that resulted in an overall weaker plant response. Results indicated that applied N in soil where there is a nutrient deficiency, likely is not absorbed by rice plants and can be susceptible to nitrification and denitrification [27,28,50]. Additionally, soil in the UC likely maintained greater soil moisture compared to the other fertilizer-P treatments due to the lower water demand from stunted plants, which would have increased the duration of time in which conditions optimal for N₂O production occurred. Slayden, et al. [13] reported season-long N₂O emissions that ranged from 0.42 kg N₂O ha⁻¹ season⁻¹ from an UC that received no N to 0.65 kg N₂O ha⁻¹ from optimally N fertilized rice with one additional split application. Season-long N₂O emissions reported by Slayden, et al. [13] were smaller than that reported in the current study, as rice plants received, at most, 63% of the N applied in the current study compared to what was applied in Slayden, et al. [13]. In contrast, season-long N₂O emissions reported by Slayden, et al. [46] were roughly double that from the current study for furrow-irrigated rice grown on a silt-loam soil near Stuttgart, AR. At the field scale, Della Lunga, et al. [27] reported season-long N₂O emissions from six fertilizer-P treatments, including $\mathsf{ECST}_\mathsf{Syn}$ and CPST, that were similar in both magnitude and trend among fertilizer-P treatments. Furthermore, N₂O emissions from the P-fertilized treatments in the current study were similar to both the up- (1.9 kg ha⁻¹) and down-slope (1. kg ha-1) field positions reported by Timms, et al. [54] during the 2020 to 2021 growing season for the hybrid rice variety XP 117. Additionally, both the current study and Timms, et al. [54] reported peak N₂O emissions immediately following N fertilizer applications followed by near zero values for the remainder of the growing season, emphasizing the loss potential of N, especially in the up-slope field position that was most similar to the soil conditions in the current study. Karki, et al. [55] reported season-long N₂O emissions of 7.4 and 1.5 kg N₂O-N ha⁻¹ from the up- and downslope field positions in an Arkansas furrow-irrigated rice field. Similar results from both Karki, et al. [55] and Timms, et al. [54] regarding season-long $\rm N_2O$ emissions reinforces the characterization that the soil conditions of the current study were most comparable to the up-slope position of a furrow-irrigated rice field and that oscillating soil moisture conditions present in the up-slope position pose an enhanced potential for N loss. The notable difference in $\rm N_2O$ emissions between studies emphasizes the large range in potential N loss from furrow-irrigated rice and the importance of proper N and irrigation management, as gaseous-N losses harm both crop productivity and increase overall GWP.

Similar to CH₄ and N₂O, season-long CO₂ emissions in the current study were comparable to that reported by Della Lunga,et al. [27,28]. The lack of difference between the struvite-P sources and MAP, likely indicates that, over a growing season, the struvite-P sources performed as an efficient-P source that was similar to MAP, a widely used and commercially available fertilizer-P source from rice and other crops. In Arkansas, the efficient use of ECST as a fertilizer-P source, without a loss in agronomic productivity, has been reported in flood-irrigated rice, soybean (Glycine max), and corn (Zea mays) [23-25]. Both Omidire, et al. [24] and [25] studies in which ECST was compared to numerous other commercially-available, commonly-used fertilizer-P sources via agronomic response reported significantly improved corn and numerically greater soybean yields, respectively, compared to at least one other non-struvite fertilizer-P source. Furthermore, in a floodirrigated rice system in Arkansas, Omidire, et al. [23] reported no difference between fertilizer-P sources regarding yield during the 2019 growing season and only a minor decrease in yield from ECST (11 Mg ha⁻¹) compared to TSP (13.1 Mg ha-1), while the majority of other measured plant properties did not differ among fertilizer-P sources across two growing seasons. The decreased season-long CO₂ emissions reported for the UC suggested how suboptimal-P fertilization can have a substantial impact on soil fertility, agronomic production and environmental assessment of crop systems.

Although total GWP did not differ among P-fertilized treatments, MAP was numerically largest, followed by the struvite-P sources. The large water solubility of MAP likely resulted in a faster release of nutrients early in the growing season that stimulated respiration from both plants and the soil. Averaged across treatments, season-long $\mathrm{CH_4}$, $\mathrm{N_2O}$, and $\mathrm{CO_2}$ emissions represented 0.1, 3.3, and 96.6% of the total GWP, respectively, supporting the need for the $\mathrm{CO_2}$ -excluded GWP. as the total GWP was similar to season-long $\mathrm{CO_2}$ emissions, masking potential trends for $\mathrm{CH_4}$ and $\mathrm{N_2O}$ that can provide essential information to develop mitigation practices (Table 5).

Previously, the focus of research on reducing the GWP of rice production has focused on CH_4 and N_2O due to the impracticality of limiting plant and soil respiration [49]. Averaged across treatments, season-long N_2O emissions represented 97.2% of CO_2 -excluded GWP, which was a similar proportion to that reported by Della Lunga, et al. [27], stressing that the focus of GHG management in furrow-irrigated rice should on N_2O reduction and proper N management.

Conclusions

The current study investigated the effects of various fertilizer phosphorus treatments on greenhouse gas emissions in a simulated furrow-irrigated rice production system in a controlled greenhouse environment. The greenhouse gas fluxes differed among treatments over time, but in contrast to that hypothesized, the greatest methane flux did not occur from monoammonium phosphate, but occurred from the chemically precipitated struvite. In contrast to that hypothesized, the peak methane flux from the phosphorusfertilized treatments did not show a temporal pattern related to the solubility of the P-fertilizers. In contrast to that hypothesized, season-long methane emissions did not differ among fertilizer-P treatments. As was hypothesized, seasonlong nitrous oxide emissions differed among fertilizer-P sources and were greatest from the unamended control. Similarly, season-long carbon dioxide emissions were, as hypothesized, smallest from the unamended control. In contrast to season-long methane emissions, but similar to season-long carbon dioxide emissions, total global warming potential differed among fertilizer phosphorus sources and was smallest from the unamended control. Contrary to total global warming potential, the carbon dioxide-excluded global warming potential differed among fertilizer phosphorus treatments and was greatest from the unamended control.

Future challenges associated with the intensification of climate change, globally decreasing phosphorus supplies, and rice production in furrow-irrigated systems have warranted both the current study and future studies to improve understanding of how the use of water-saving production systems, like furrow-irrigation, in conjunction with alternative fertilizer phosphorus sources, such as struvite, can improve the sustainability of food production. The current study concluded that the use of wastewater-derived, electrochemicallyprecipitated struvite was similar in season-long emissions and global warming potentials to the other struvite fertilizer sources and the widely used, commercially available monoammonium phosphate fertilizer, emphasizing both the scalability of the electrochemically-precipitated struvite product to real-world production and the comparability wastewater-derived, electrochemically-precipitated struvite products to previous research on syntheticallyderived, electrochemically-precipitated struvite. As a result, wastewater-derived, electrochemically-precipitated struvite could decrease the season-long emissions and GWP of furrow-irrigated production in Arkansas without sacrificing agronomic productivity.

Further research into the use of wastewater-derived, electrochemically precipitated struvite at the field-scale, both independently and in conjunction with management practices intended to reduce greenhouse gas emissions, is one of the next logical steps in struvite research. With the expected increase in furrow-irrigated rice production in Arkansas, research into how the use of struvite to reduce nitrous oxide emissions is warranted to further reduce the global warming potential of furrow-irrigated rice systems. Additionally, field-scale studies into how the use of struvite as an alternative fertilizer phosphorus source impacts runoff

water quality could further bolster the benefits associated with struvite use.

Acknowledgments

This work was supported by a grant from the USDA-NIFA-AFRI Water for Food Production Systems program (Award # 2018-68011-28691).

References

- Cordell D, Drangert J, White S (2009) The story of phosphorus: Global food security and food for thought. Glob Environ Change 19: 292-305.
- Intergovernmental Panel on Climate Change (IPCC), (2021) Global carbon and other biogeochemical cycles and feedbacks. In: Canadell JG, Monteiro PMS, Costa MH, et al. Climate Change 2021: The Physical Science Basis. Contribution of Working Group I to the Sixth Assessment Report of the Intergovernmental Panel on Climate Change, Cambridge University Press, United Kingdom, 673-816.
- United States Environmental Protection Agency (USEPA) (2022) Inventory of US Greenhouse Gas Emissions and Sinks: 1990-2020.
- Fraiture CD (2007) Future water requirements for foodthree scenarios, International Water Management Institute (IWMI), seminar: water for food, bio-fuels for ecosystems? World water week 2007. Stockholm, Sweden.
- Brady NC, Weil RR (2016) The nature and properties of soils (15th edn). Pearson, London
- 6. Liu XJ, Mosier AR, Halvorson AD, Reule CA, Zhang FS (2007) Dinitrogen and $\rm N_2O$ emissions in arable soils: Effect of tillage, N source and soil moisture. Soil Bio Biochem 39: 2362-2370.
- Dubey SK (2005) Microbial ecology of methane emission in rice agroecosystem: A review. Applied Ecol Environ Res 3: 1-27.
- 8. Hardke J, Sha X, Bateman N (2022) Trends in Arkansas rice production, 2021. In: BR Wells Arkansas Rice Research Studies 2021. Arkansas Agricultural Experiment Station Research Series, 685. Arkansas, 11-18.
- Henry CG, Hirsch SL, Anders MM, et al. (2016) Annual irrigation water use for Arkansas rice production. J Irrig Drain Eng 142: 05016006. https://doi.org/10.1061/(ASCE) IR.1943-4774.0001068
- He C (2010) Effects of furrow irrigation on the growth, production, and water use efficiency of direct sowing rice. Sci World J 10: 1483-1497. https://doi.org/10.1100/ tsw.2010.146
- 11. Rector C, Brye KR, Humphreys JJ, et al. (2018) $\rm N_2O$ emissions and global warming potential as affected by water management and rice cultivar on an Alfisol in Arkansas, USA. Geoderma Reg 14: e00170.
- Rector C, Brye KR, Humphreys J, et al. (2018) Tillage and coated-urea effects on nitrous oxide emissions from directseeded, delayed-flood rice production in Arkansas. J Rice Res Dev 1: 25-37.
- Slayden JM, Brye KR, Della Lunga D (2022) Nitrogen fertilizer application timing effects on nitrous oxide emissions from simulated furrow-irrigated rice on a siltloam soil in the greenhouse. J Rice Res Dev 5: 366-377.

- Della Lunga D, Brye KR, Slayden JM, et al. (2020) Soil moisture, temperature, and oxidation-reduction potential fluctuations across a furrow-irrigated rice field on a siltloam soil. J Rice Res Dev 3: 103-114.
- Della Lunga D, Brye KR, Slayden JM, et al. (2021) Relationships among soil factors and greenhouse gas emissions from furrow-irrigated Rice in the mid-southern, USA. Geoderma Reg 24: e00365.
- Hardke JT, Chlapecka JL, (2020) Arkansas Furrow-Irrigated Rice Handbook. University of Arkansas, Division of Agriculture, Cooperative Extension Service (UA-DA-CES), Little Rock, AR.
- 17. Holford ICr (1997) Soil phosphorus: its measurement, and its uptake by plants. Aust J Soil Res 35: 227-240.
- 18. Shen J, Yuan L, Zhang J, et al. (2011) Phosphorus dynamics: From soil to plant. Plant Physiol 156: 997-1005.
- Prasad R, Shivay YS, Majumdar K, et al. (2016) Phosphorus management. In: Rattan L, Stewart BA, Soil phosphorus advances in soil science. CRC Press, Florida, 81-114.
- Muhmood A, Lu J, Dong R, et al. (2019) Formation of struvite from agricultural wastewaters and its reuse on farmlands: Status and hindrances to closing the nutrient loop. J Environ Manag 230: 1-13.
- Schoumans OF, Bouraoui F, Kabbe C, et al. (2015) Phosphorus management in Europe in a changing world. Ambio 44: S180-S192.
- 22. Ylagan S, Brye KR, Greenlee L (2020) Corn and soybean response to wastewater-recovered and other common phosphorus fertilizers. Agrosyst Geosci Environ 3: e20086.
- 23. Omidire NS, Brye KR, Roberts TL, et al. (2021) Evaluation of electrochemically precipitated struvite as a fertilizer phosphorus source in flood ☐ irrigated rice. Agron J 114: 739-755.
- Omidire NS, Brye KR, English L, et al. (2022) Wastewater □ recovered struvite evaluation as a fertilizer □ phosphorus source for corn in eastern Arkansas. Agron J 114: 2994-3012.
- Omidire NS, Brye KR, English L, et al. (2022) Soybean growth and production as affected by struvite as a phosphorus source in eastern Arkansas. Crop Sci 63: 320-335
- 26. Omidire NS, Brye KR (2022) Wastewater □recycled struvite as a phosphorus source in a wheat-soybean double □crop production system in eastern Arkansas. Agrosyst Geosci Environ 5: e20271.
- 27. Della Lunga D, Brye KR, Roberts TL, et al. (2024) Struvitephosphorus effects on greenhouse gas emissions and plant and soil response in a furrow-irrigated rice production system in eastern Arkansas. Front Clim 6: 1342896.
- 28. Della Lunga D, Brye KR, Roberts TL, et al. (2024) Water regime and fertilizer-phosphorus source effects on greenhouse gas emissions from rice. Agrosyst Geosci Environ 7: e20482.
- Chien SH, Prochnow LI, Tu S, et al. (2011) Agronomic and environmental aspects of phosphate fertilizers varying in source and solubility: An update review. Nutr Cycl Agroecosystems 89: 229-255.

- 30. Hertzberger AJ, Cusick RD, Margenot AJ (2020) A review and meta-analysis of the agricultural potential of struvite as a phosphorous fertilizer. Soil Sci Soc Am J 84: 653-671.
- United States Division of Agriculture Natural Resources Conservation Services (USDA-NRCS) (2018) Calhoun soil series.
- 32. Gee GW, Or D (2002) Particle size analysis. In: Dane JH, Topp GC, Methods of soil analysis, part 4: physical methods. Series 5, Wiley, New York, 255-293.
- 33. Tucker MR (1992) Determination of phosphorus by Mehlich 3 extraction. In: Soil and media diagnostic procedures for the southern region of the United States, southern cooperative series bulletin no. 374. Virginia Agricultural Experiment Station Series.
- 34. Nelson DW, Sommers LE (1996) Total carbon, organic carbon, and organic matter. In: Sparks DL, Page AL, Helmke PA, Loepper RH, Soltanpour PN, Tabatabai MA, Johnston CT, Sumner ME, Methods of soil analysis. Part 3: Chemical analysis, (3rd edn), Soil Science Society of America, Wisconsin, 961-1010.
- 35. Hardke JT (2021) Rice Production Handbook. University of Arkansas, Division of Agriculture, Cooperative Extension Service (UA-DA-CES), Little Rock, AR.
- 36. Ostara Nutrient Recovery Technologies Inc (2020) Nutrients.
- 37. Kékedy-Nagy L, Teymouri A, Herring AM, et al. (2020) Electrochemical removal and recovery of phosphorus as struvite in an acidic environment using pure magnesium vs. the AZ31 magnesium alloy as the anode. Chem Eng J 380: 122480.
- 38. United States Environmental Protection Agency (USEPA) (1996) Method 3050B: Acid Digestion of Sediments, Sludges, and Soils, Revision 2. Washington, DC.
- Brye JB, Della Lunga D, Brye KR (2024) Rice response to struvite and other phosphorus fertilizers in a phosphorusdeficient soil under simulated furrow-irrigation. J Soil Sci Plant Nutr 24: 7491-7506.
- 40. University of Arkansas, Division of Agriculture, Cooperative Extension Service (UA-DA-CES) (2023) Rice Management Guide. UA-DA-CES, Little Rock, AR.
- 41. Bouman BAM, Tuong TP (2001) Field water management to save water and increase its productivity in irrigated lowland rice. Agric Water Manag 49: 11-30.
- 42. Sander BO, Wassmann R (2014) Common practices for manual greenhouse gas sampling in rice production: A literature study on sampling modalities of the closed chamber method. Greenh Gas Meas Manag 4: 1-13.
- 43. Humphreys JJ, Brye KR, Rector C, et al. (2018) Water management and cultivar effects on methane emissions from direct-seeded, delayed-flood rice production in Arkansas. J Rice Res Dev 1: 14-24.
- 44. Humphreys JJ, Brye KR, Rector C, et al. (2018) Methane production as affected by tillage practice and NBPT rate from a silt-loam soil in Arkansas. J Rice Res Dev 1: 49-58.
- 45. Rogers CW, Brye KR, Smartt AD, et al. (2014) Cultivar and previous crop effects on methane emissions from drill-seeded, delayed-flood rice production on a silt-loam soil. Soil Sci 179: 28-36.

Citation: Arel CM, Brye KR, Lunga DD, et al. (2025) Struvite Effects on Greenhouse Gas Emissions from Furrow-irrigated Rice in the Greenhouse. J Rice Res Dev 7(1):491-503

- 46. Slayden JM, Brye KR, Della Lunga D, et al. (2022) Site position and tillage treatment effects on nitrous oxide emissions from furrow-irrigated rice on a silt-loam Alfisol in the Mid-south, USA. Geoderma Reg 28: e00491.
- Smartt AD, Brye KR, Rogers CW, et al. (2016) Previous crop and cultivar effects on methane emissions from drillseeded, delayed-flood rice grown on a clay soil. Appl Environ Soil Sci 2016: 1-13.
- 48. Intergovernmental Panel on Climate Change (IPCC) (2014) Climate change 2014: Impacts, adaptation, and vulnerability. Part A: Global and Sectoral Aspects, working group II contribution to the fifth assessment report. Cambridge University Press, Cambridge.
- Paustian K, Cole CV, Sauerbeck D, et al. (1998) CO₂ mitigation by agriculture: an overview. Clim Change 40: 135-162.
- Arel C (2024) Struvite effects on greenhouse gas emissions from flood- and furrow-irrigated rice in the greenhouse. In: Graduate Theses and Dissertations, University of Arkansas.

- 51. Lu Y, Wassmann R, Neue HU, et al. (1999) Impact of phosphorous supply on root exudation, aerenchyma formation and methane emission of rice plants. Biogeochem 47: 203-218.
- 52. Della Lunga D, Brye KR, Slayden JM, et al. (2023) Evaluation of site position and tillage effects on global warming potential from furrow-irrigated rice in the midsouthern USA. Geoderma Reg 32: e00625.
- 53. Humphreys J, Brye KR, Rector C, et al. (2019) Methane emissions from rice across a soil organic matter gradient in Alfisols of Arkansas, USA. Geoderma Reg 16: e00200.
- 54. Timms PA, Scivittaro WB, Parfitt JMB, et al. (2025) A novel irrigation system to reduce methane emissions in paddy fields. Nut Cyc Agroecosys 130: 299-312.
- 55. Karki S, Adviento-Borbe MAA, Massey JH, et al. (2021) Assessing seasonal methane and nitrous oxide emissions from furrow-irrigated rice with cover crops. Agri 11: 261.

DOI: 10.36959/973/449

Copyright: © 2025 Arel CM. This is an open-access article distributed under the terms of the Creative Commons Attribution License, which permits unrestricted use, distribution, and reproduction in any medium, provided the original author and source are credited.

